IEEE Access
Multidisciplinary | Rapid Review | Open Access Journal

Received April 2, 2022, accepted May 8, 2022, date of publication May 17, 2022, date of current version June 6, 2022.

Digital Object Identifier 10.1109/ACCESS.2022.3175861

End-to-End PSK Signals Demodulation Using Convolutional Neural Network

WEN-JIE CHEN[1], JIAO WANG[2], AND JIAN-QING LI[2], (Member, IEEE)
[1]Southwest China Institute of Electronic Technology, Chengdu 610036, China
[2]School of Electronic Science and Engineering, University of Electronic Science and Technology of China, Chengdu 611731, China
Corresponding author: Jian-Qing Li (lijq@uestc.edu.cn)

ABSTRACT Demodulation techniques are of central importance for achieving intelligent receiving. Improvement in demodulation performance enhances the overall performance of a communication system correspondingly. However, conventional demodulators require dedicated hardware platforms leading to high implementation costs and time-consuming development. This work proposes a unified architecture for end-to-end automatic demodulated modulated signals. The proposed demodulator utilizes the residual unit and fully convolutional network (R-FCN) to extract the time-domain feature of the modulated signal and determine the transmitted symbols to realize the demodulation of a received signal. Simulations show that the proposed method has better demodulation performance compared to existing methods. It is further demonstrated that when the signal-to-noise ratios (SNR) exceed 2dB, the proposed demodulator exhibits similar demodulation performance to symbol-unsynchronized data compared to conventional demodulators.

INDEX TERMS Convolutional neural network, demodulation, residual network.

I. INTRODUCTION

Phase shift keying (PSK) is a digital modulation scheme that transmits information by shifting the carrier wave between different phases. In a pure PSK, both the amplitude and the frequency of the transmitted carrier are typically kept constant [1]. Because PSK is more efficient and less prone to errors than frequency shift keying (FSK) and other modulation forms. It is used extensively in digital microwave communication, mobile communication, satellite communication, broadband access, and cable television systems [2]. The current research for wireless communication systems mainly starts with accurate and high energy efficiency or high spectrum utilization, while signal demodulation directly impacts wireless transmission performance.

With the rapid development of computer science and hardware, machine learning has been developed accordingly. Deep learning (DL) [3] is a sub-class of machine learning (ML) that focuses on utilizing convolutional neural networks (CNNs) to extract helpful features in raw data automatically. Inspired by the architecture and functionality of the artificial neural networks (ANN), deep learning uses algorithms to learn abstract features directly from input data in a hierarchical manner with features from higher levels of the hierarchy formed by the composition of lower-level features. Researchers have been exploring its use in communication fields since the introduction of DL [4]. Currently, DL has been applied to channel estimation [5], [6], modulation recognition [7]–[9], channel code recognition [10], [11], communication system simulation [12], [13] and decoding [14]–[16].

Signal demodulation based on learning methods has been widely studied in recent years, and the application of neural networks is more common than other algorithms such as support vector machines (SVM). Depending on the data processing method, the signal demodulation methods can be divided into the sampling points grouping-based and the phase shifts detecting-based. According to the different neural network models used, the signal demodulation methods can be divided into four types: multilayer perceptron (MLP) [18]–[20], deep belief network (DBN) [21], long short-term memory (LSTM) [22], and CNN [25]–[28]. In [17], an ANN demodulator was proposed to demodulate the FSK signal. It can efficiently demodulate the FSK signal transmitted in a complex noise context and significantly enhance the anti-interference capability. And Kaizhi and Hu [23] presented a pattern recognition theory-based PSK demodulation algorithm that recognizes PSK order and simultaneously eliminates phase shift interference. The

The associate editor coordinating the review of this manuscript and approving it for publication was Wei Wang.

authors from [19] designed an electrocommunication system for deep learning-based demodulation. In [21], two data-driven frameworks of signals demodulation techniques, including the DBN-SVM-based approach and the adaptive boosting (AdaBoost)-based approach, are summarized. In [22], the LSTM unit-aided intelligent deep neural network (DNN)-based DL demodulator was proposed to demodulate the received signals. Better performance than the benchmark systems was obtained. Elbaz and Zibulevsky [24] proposed to employ the prior information of transmitted speech messages to train a DNN and LSTM for Frequency modulation (FM) demodulation. Onder *et al.* [20] considered that wireless channels often got substantial interference. So, they designed a feedforward neural network demodulator to demodulate the transmitted signal over unknown channels. The network was pre-trained with pilot signal then further trained in multipath transmission scenario. It obtained better BER performance in the Rayleigh channel than the traditional correlation demodulator.

Recently, many researchers applied CNN to resolve the digital modulation signals' demodulation problems (see, e.g.,[25]–[28]). The authors in [25] proposed three ML demodulators based on CNN, the DBN, and AdaBoost. Particularly, the CNN-based demodulator transforms the modulated signal into an image and identifies the demodulation symbols of the received signal by the image classification. In [27], the mixed-signal demodulation was investigated based on the deep convolutional network. This method attempts to demodulate symbol sequences from mixing signals, respectively. However, all aforementioned methods need to take samples at each symbol period as the input to their neural networks, and then they use neural networks to binarize them. Nevertheless, grouping the baseband data strictly according to the symbol period is challenging to achieve, primarily when frequency offset or sampling error occurs. To address this issue, Zhang *et al.* [26] proposed the 1-D CNN-based binary phase-shift keying (BPSK) demodulator, which uses 1-D CNN to detect the location and form of the phase jump of the BPSK signal, thereby obtaining the demodulation results. This method needs neither complicated preprocessing nor sample sequence grouping, yet an increase in the number of phase jumps will call for a corresponding rise in the number of CNNs that need to be built. Therefore, this approach is no longer practical when the modulation order is raised.

We can see that CNN is a widely used neural network model for signal demodulation from the above. For the most part, in CNN-based signal demodulation approaches, the input vector of received signal supported by the CNN is frequently required grouping of the sampling sequences. Then a CNN model is used to demodulate the modulated signal within one sampling period into one symbol. However, as the number of modulating orders increases, the number of categories increases exponentially. With the aid of the residual network, we first use the entire modulated signal as input to the CNN demodulator instead of a single symbol period to solve the sampling points grouping problem. Subsequently, we use N multi-category classifiers at the final classification layer to demodulate N symbols information stream instead of a single binary classifier.

This paper presents a residual unit and fully convolutional networks (R-FCN)-based end-to-end demodulator, which can be applied to different modulation schemes with a few modifications. This approach allows learning and extracting features directly from the received modulated signal without any a *priori* knowledge of the channel model. As a comparison, MLP, LSTM, CNN, and the conventional methods are also studied. Then, we investigate the BER of BPSK, QPSK, and 8PSK signals with different SNRs. In order to train the model, three modulate signals of single-carrier modulated signal samples with additive white gaussian noise (AWGN) are generated in various SNR circumstances. Furthermore, we investigate how symbol-unsynchronized data affect the demodulation performance for QPSK signals. Results show that the proposed demodulator is relatively insensitive to symbol-unsynchronized data compared to conventional algorithms.

The rest of this paper is organized as follows. Section II briefly introduces the signal model and a typical CNN model. Section III gives a description of the presented CNN demodulator in detail. The results of the experiment and performance analysis are given in Section IV, and the conclusion in Section V.

II. BACKGROUND

A. SYSTEM MODEL

As shown in Fig. 1, this PSK signal transmission system consists of three main parts, a transmitter, a transmission channel, and a receiver. The transmitter comprises a baseband modulator, a baseband-shaping filter, and a carrier wave modulator [29]. The receiver is composed of a preprocessor and a neural network demodulator. At the transmission end, after baseband modulation, baseband-shaping filtering, and carrier wave modulation, the information bits that have turned into an intermediate frequency (IF) signal is then up-conversed into a high frequency (HF) signal, which is more suitable for channel transmission. In the transmission channel, AWGN is added to the transmission signal. The receiving signal is first down-converted into an IF signal at the receiving end. Next, it is preprocessed then sent to the neural network to get the demodulated information bits.

PSK is a digital modulation process that transmits information by shifting the carrier wave between different phases. This paper focuses on studying modulated signals demodulation corrupted by additive white Gaussian noise (AWGN). We suppose that the transmitted information bitstream is independent identically distributed (*i.i.d.*) and that the transmitter uses the PSK signal waveform to send digital information. When the PSK digital modulation scheme is used, the transmitted signal x(t) is expressed as

$$x(t) = A\cos(2\pi f_c t + w_n), n = 1, \ldots, M \tag{1}$$

where A denotes the amplitude, f_c is the carrier frequency of the modulated signal, w_n is the absolute phase of the *n-th*

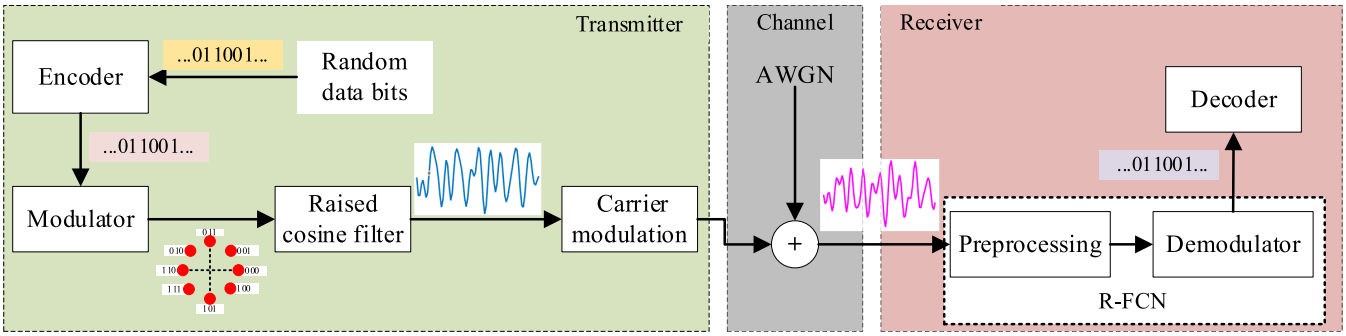

FIGURE 1. The system model based on residual networks and fully convolutional networks demodulator of PSK signal under AWGN channel.

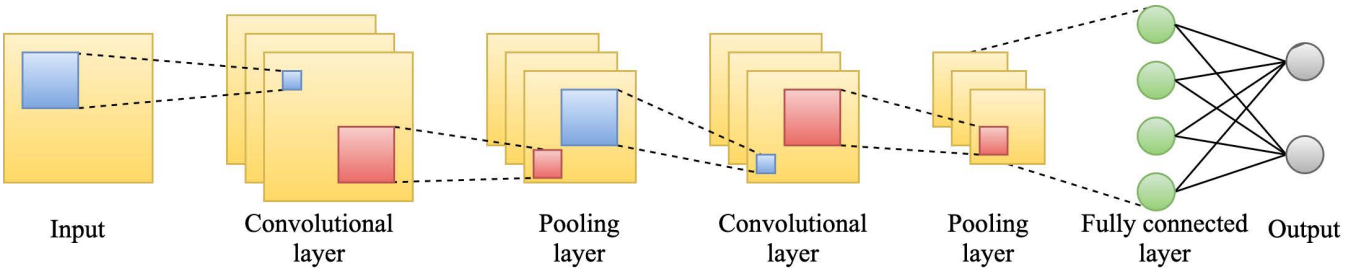

FIGURE 2. A typical CNN consists of an input layer, convolutional layers, pooling layers, and an output layer.

symbol. M is the modulation order. Each symbol of MPSK modulation corresponds to k bits, and there are M symbols in total.

At the receiver, the received signal $y(t)$ in the communication system is given by:

$$y(t) = x(t) * c(t) + n(t) \tag{2}$$

where $x(t)$ represents the transmitted pulse-shaped signal, $c(t)$ is the channel pulse response, and $n(t)$ denotes AWGN noise with power σ_n^2.

B. CONVOLUTIONAL NEURAL NETWORK

CNNs are artificial neural networks that are so far generally used to analyze visual images [30]. Inspired by early findings in the study of biological vision, a typical CNN consists of an input layer, convolutional layers, pooling layers, and an output layer, as shown in Fig. 2.

As the most critical module in the CNN, the convolutional layer is vital in applying the model. The parameters of the neural network consist of a set of learnable convolutional kernels, all of which are set as a small receptive field and then expanded to the entire input data by means of a sliding window convolution. During forward propagation, each convolution kernel computes the dot product of the filter with the previous layer of input in the width and height directions of the input data, and then generates a two-dimensional activation map for that convolution kernel. The convolution operation can be expressed as:

$$u_i^l = f\left(\sum_{j=1}^{m} w_j^l \times u_{i-j+m}^{l-1} + b^{(l)}\right) \tag{3}$$

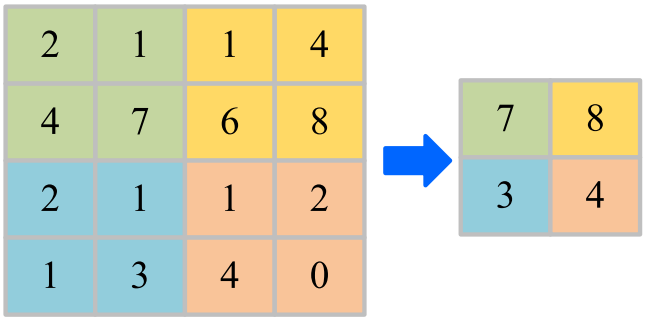

FIGURE 3. Max pooling with a 2 × 2 filter and stride = 2.

where w_j^l and b_j^l represent the weights and bias of the l-th convolution kernel, respectively, and $f(\cdot)$ represents the activation function.

Another important concept of CNNs is pooling. A pooling layer is a nonlinear down-sampling layer, and it is often added after the convolutional layers to reduce the dimensionality of the feature map. Pooling operation increases the receptive field's size and helps make a representation approximately invariant to local translation. Two standard functions used in the pooling operation are average pooling and max pooling which help extract background and textures, respectively, where max pooling is the most common (see Fig. 3). When the background is noisy or complicated, max pooling is usually used to summarize the most activated presence of a feature.

C. RESIDUAL NETWORK

As the depth of a convolutional neural network grows, the gradient of the loss function approaches zero, leading to

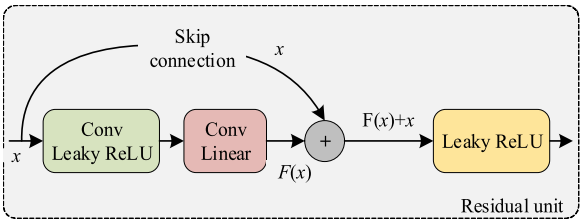

FIGURE 4. The residual unit.

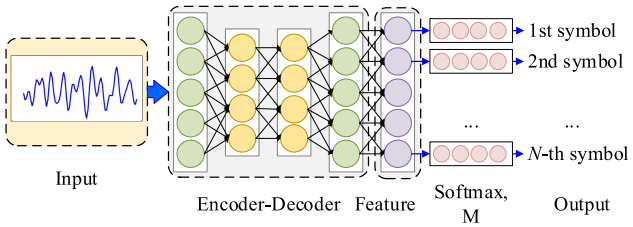

FIGURE 5. Architecture of the CNN-based demodulator.

higher training error. To address this problem, He *et al*. [31] presented a residual learning framework (ResNet). A residual neural network (ResNet) is an artificial neural network (ANN) that builds on the known structure of cortical pyramidal cells. Residual neural networks do this by skipping connections or shortcuts to skip specific layers. A typical ResNet model is accomplished by double- or triple-layer skip connections, which includes rectified linear unit (ReLU)) and batch normalization (BN) in between.

A residual unit is shown in Fig. 4. Denoting the input of the residual unit as x and output as $H(x)$, unlike plain CNN, which tries to learn the actual output $H(x)$, Residual networks learn the residual–$F(x) = H(x)$-x. Formally, a residual unit for a ResNet is defined as:

$$x_{k+1} = \text{Leaky ReLU}(F(x_k) + x_k) \tag{4}$$

where x_k is the input of the k-*th* residual unit, and x_{k+1} is the output of the k-*th* residual unit. Leaky ReLU represents the activation function, i.e., $\sigma(x) = \max(0, x + \beta \cdot \min(0, x)$, where β is a small constant, such as 0.1 [32].

III. THE PROPOSED APPROACH

In this section, we first introduce the architecture of the proposed demodulator network in brief. Then, we describe in detail the end-to-end R-FCN demodulator architecture and give an optimized training scheme. Finally, the methods of modulation and the parameters of experimental signals are provided.

A. ARCHITECTURE OF THE PROPOSED DEMODULATOR

Fig. 5 describes the structure of the proposed CNN-based demodulator that consists of an input layer, feature extraction, classification layer, and output layer. In the input layer, the signal time-domain waveform of the received signal is input. The task of the feature generator is to extract feature maps automatically from the signal time-domain waveform of the received signal. The feature maps are used as the input of the classification layer. Multiple multi-category classifiers are used in the final classification layer to implement the received signal demodulation. Each multi-category classifier demodulates one of the symbols. The number of classifiers corresponds to the number of symbols in the signal to be demodulated.

TABLE 1. Proposed R-FCN demodulator structure.

Module	Layer	Output size
Input	Input	4096×1
Encoder	Max pooling Res stack	2048×32
	Max pooling Res stack	1024×32
	Max pooling Res stack	512×32
	Max pooling Res stack	256×32
Decoder	Up-sampling Res stack	512×32
	Up-sampling Res stack	1024×32
	Res stack	1024×32
	Res stack	1024×32
Output	Conv + Softmax	1024×M

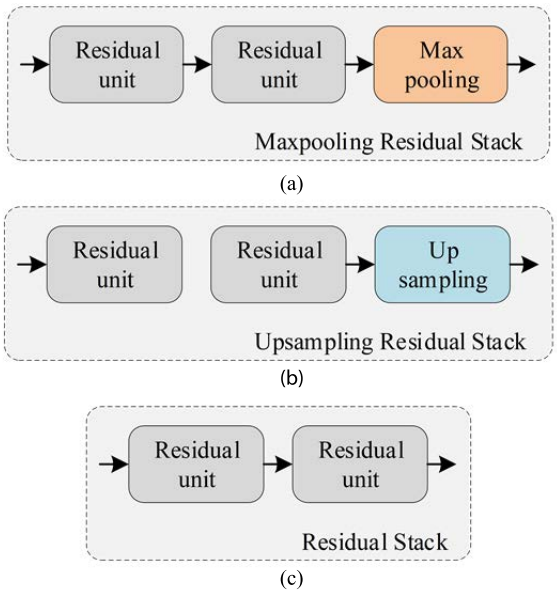

FIGURE 6. The residual stacks: (a) The max-pooling residual stack, (b) The up-sampling residual stack, (c) The residual stack.

B. PROPOSED R_FCN STRUCTURE

The proposed R-FCN demodulator consists of an input layer, an encoder, a decoder, and an output layer. See Table 1 for detailed architecture. There are 4096 nodes in the input layer, the same length as the input vector. The encoder comprises four max-pooling residual stacks. Fig. 6*a* shows the architecture for the max-pooling residual stack, consisting of two residual units and a max-pooling layer. The encoder performs convolution and max-pooling operations to extract and summarize features. The obtained feature maps are then sent to the decoder.

As shown in Figs 6, the decoder comprises two up-sampling residual stacks and two residual stacks. In this work, the number of samples per symbol have a fixed number of 4. Thus, there are two more max-pooling layers in the demodulator than the number of up-sampling layers, and two more max-pooling layers are used to down-sample the incoming signals. When changing the number of sample points, the architecture of the demodulator changes correspondingly. The output layer contains only a single convolutional layer. Its output indicates the demodulation results for the incoming signals, whose dimension is determined by the modulation order (M). The output length is calculated by the input length and the number of samples per symbol.

During training, optimizations are made for a CNN better to fit the communication signal demodulation task [34]. First, we use Leaky ReLU [32] as the nonlinear activation function after each convolutional layer. It allows faster convergence than traditional nonlinear activation functions and doesn't omit negative values compared to ReLU. However, the activation function used in the demodulation layer is the Softmax function so that the output values of each Softmax function can be controlled in the [0,1] interval. Since the activation function used in the demodulation layer is different from the other layers, the Xavier initialization method [33] is used to initialize the weights to ensure the consistency of the input and output variances throughout the network. Second, the batch normalization [35] technique is used after each convolution layer to make its output (input for the next layer) follow a standard distribution, improving the generalization performance.

C. DATASETS

The size and variety of the dataset significantly impact the effectiveness of deep learning techniques. This paper evaluates the proposed demodulation algorithm on three widely used digital modulation schemes-BPSK, QPSK, and 8PSK. We use MATLAB to generate random binary bitstreams then modulate them with the above three modulation schemes. In our experiments, we set the frequency of carrier wave f_c at 23.325KHz, the sampling rate f_s at 93.3KHz. We select 23.325Kbps of symbol rate to obtain the most sampling points. In addition, we add AWGN to signals to train the demodulator, which attributes to the enhancement of noise immunity. The channel SNR is calculated by the ratio of energy per symbol to the spectral noise density (E_s/N_0) and oversampling factor. The relationship between E_s/N_0 and SNR, both expressed in dB, is as follows:

$$SNR(dB) = E_s/N_0(dB) - 10 * \log 10(0.5^* sps) \qquad (5)$$

where sps is the number of samples per symbol (oversampling factor). For an actual input signal oversampled by a factor of 4, the E_s/N_0 exceeds the corresponding SNR by $10\times\log10(0.5^*4)$.

The data is produced from simulations in different channel SNR (−4 dB to 8 dB) environments for training sets and validation sets concerned in this work. A group of data (10000 samples, 90% for training, 10% for validation) is generated for every 2 dB of SNR change. Eight groups of data are generated in total. Due to the difference in bit error ratio (BER) among the three modulation schemes, the SNR range of the BPSK, QPSK, 8PSK test sets are set to be −5 dB to 8 dB, −5 dB to 10 dB, and −5 dB−15d B, in the order given. One thousand samples are generated for every 1 dB of SNR change for each modulation scheme.

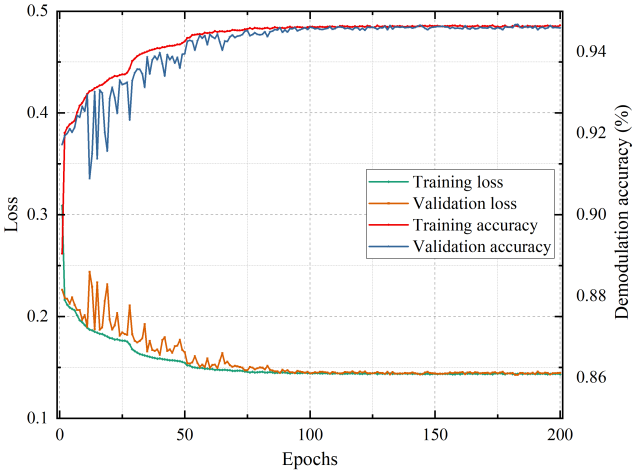

FIGURE 7. Training loss and accuracy curves vs. epoch numbers when training the R-FCN demodulator for QPSK signals.

IV. SIMULATION RESULTS

In this section, we conduct a series of simulation experiments to demonstrate the effectiveness and robustness of the proposed R-FCN demodulator.

A. TRAINING OF THE NETWORKS

The R-FCN demodulator is used to demodulate the three modulation data sets (BPSK, QPSK, and 8PSK). We train the network on the training sets, and the validation sets are partitioned in Section III. Categorical cross-entropy and Adam are used as the loss function and optimization algorithm for training, and the initial learning rate is set to be 0.001. If the verification loss is not reduced over eight epochs, the learning rate is reduced to one-tenth of the previous learning rate. In addition, the mini-batch method is used to partition the input training data sets into several batches to improve the stability of convergence. In this work, the mini-batch size is set to be 64. Fig. 7 shows the accuracy and loss value curves of the QPSK demodulation training. The horizontal axis represents the number of training epochs, the left vertical axis represents the loss value, and the right vertical axis represents the accuracy demodulation. We see that the demodulation accuracy increases with the increase of the epochs, while the loss value decreases with the rise of the periods. Moreover, both reach a stable state after about 100-epoch. The training curves for BPSK and 8PSK signals are similar. For simplicity, we will not detail them.

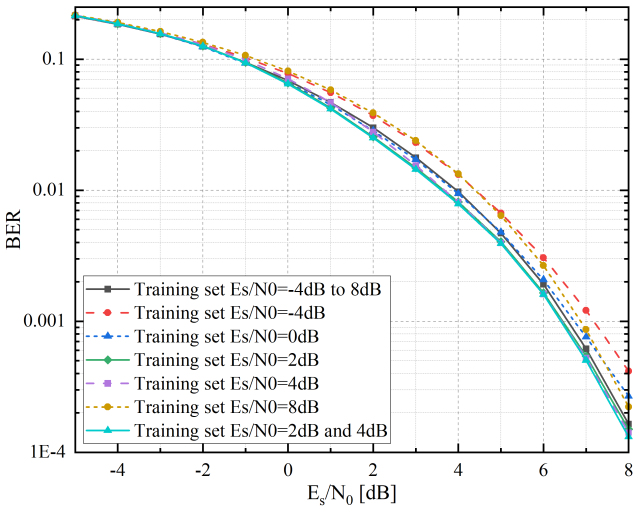

FIGURE 8. The BER performance of different training signal sets for BPSK signals.

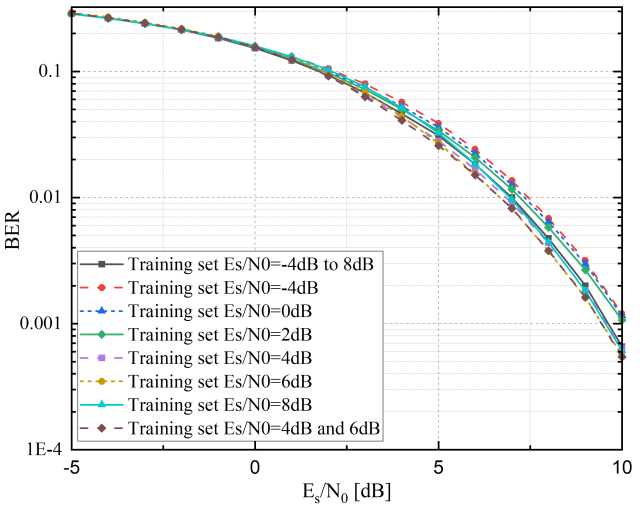

FIGURE 9. The BER performance of different training signal sets for QPSK signals.

B. IMPACT ON DATA SETS

In previous signal recognition tasks (e.g., modulation recognition, channel coding recognition), signals with all SNR levels are needed for analysis of the impact of SNR level on recognition accuracy. We use another training method to analyze the influence of SNR on BER performance in this case because the proposed CNN-based demodulation task is different from the traditional classification task. First, we train on each of the eight data groups to get eight corresponding demodulators, and then we train on all samples to get a demodulator. Those nine demodulators are used to demodulate the test data sets, respectively. Furthermore, the BER of each demodulator in different SNR circumstances is obtained. Experimental results show that the model trained on low SNR samples has a higher BER when demodulating high SNR. In comparison, the model trained on high SNR samples has a higher BER when demodulating low SNR samples. Therefore, training samples bringing two of the best-performing demodulators are combined into one training set. So, we use that set to train the tenth demodulator. Fig. 8, Fig. 9, Fig. 10 show BER performances of the R-FCN demodulators trained on three modulation schemes of training sets with different SNRs. In order to improve the readability of images, some test result curves are deleted because some demodulators have similar BER performances. Due to the difference in BER among the three modulation schemes, the SNR range of the BPSK, QPSK, 8PSK test sets are set to be -5 dB to 8 dB, -5 dB to 10 dB, and -5 dB-15 dB, in the order given.

We have three observations from Fig. 8, Fig. 9, Fig. 10. First, the difference in SNR of the training sets leads to different BER performances of the CNN demodulator. When training sets contain data with two levels of SNRs, the trained CNN demodulator has the best BER performance, which is called the optical demodulator. Second, each modulation scheme has its optimal demodulator. The optimal

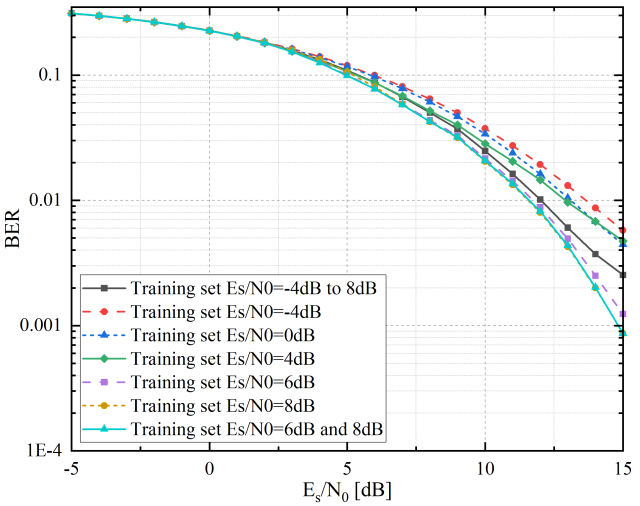

FIGURE 10. The BER performance of different training signal sets for 8PSK signals.

demodulators were obtained for BPSK, QPSK, 8PSK with SNR equal to 2 dB to 4 dB, 4 dB to 6 dB, and 6 dB to 8 dB, respectively. We can see that when the order of modulation rises, training data with higher levels of SNR are needed to yield the corresponding optimal demodulator. Last, we note that the CNN demodulator trained with all training sets has a higher BER performance than the optimal demodulators. This result indicates that higher SNR data and lower SNR data affect each other. Therefore, a suitable training set is required to obtain the desired demodulator.

C. THE PROPOSED APPROACH VERSUS OTHER DEMODULATORS

Fig. 11, Fig. 12, and Fig. 13 show the BER performance curves of the conventional demodulator, coherent demodulator, MLP demodulator [17], LSTM demodulator [22], CNN

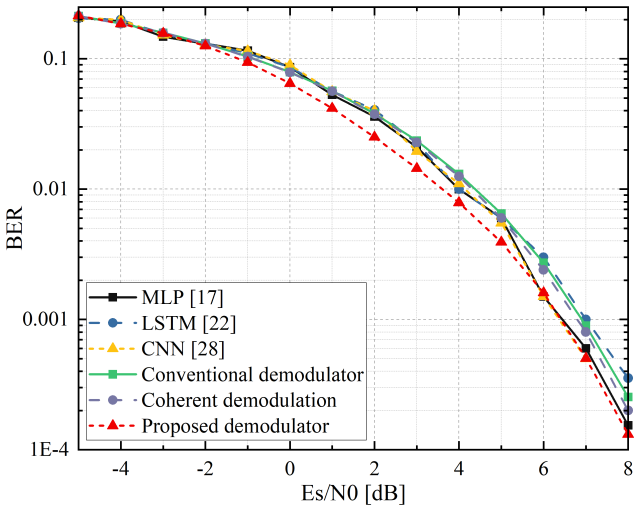

FIGURE 11. Comparison of different demodulation methods of BPSK signals in AWGN channel.

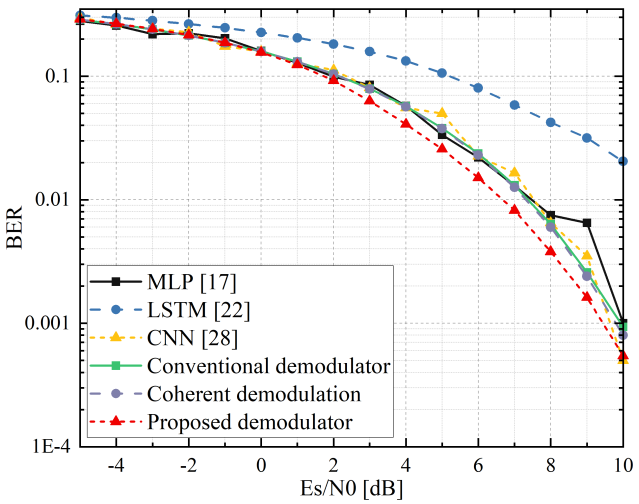

FIGURE 12. Comparison of different demodulation methods of QPSK signals in AWGN channel.

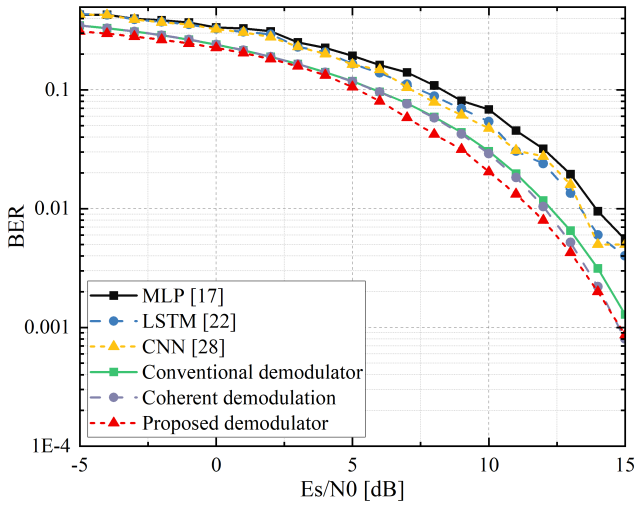

FIGURE 13. Comparison of different demodulation methods of 8PSK signals in AWGN channel.

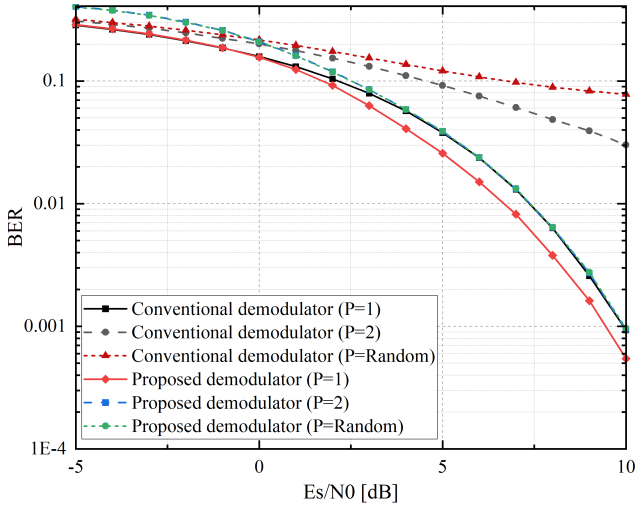

FIGURE 14. Effect of the symbol synchronization on the BER performance.

demodulator [28], and R-FCN demodulator by the demodulation of BPSK, QPSK, and 8PSK signals, respectively. All demodulators use the same training sets and test sets to make a fair comparison. As shown in Fig. 11, the BER performance of the proposed R-FCN demodulator is like the other methods when the SNR is below −1 dB and is significantly better when SNR is over 0 dB. Similarly, in Fig. 12, the BER performance of the proposed R-FCN demodulator is slightly worse than the conventional demodulator in the low SNR. Still, it outperforms other methods by about 1 dB in the high SNR. In addition, from Fig. 13, we can find that the BER performance of the LSTM demodulator is worse than the other five demodulators. It can be seen in Fig. 13 that at SNR ranges from −5 dB to 15 dB, the BER curve of the optimal R-FCN demodulator is always lower than the other three demodulators. Specifically, the proposed R-FCN demodulator can still achieve better reliability performances compared with the state-of-the-art demodulation methods.

D. EFFECT OF SYMBOL SYNCHRONIZATION

In digital communication systems, symbol synchronization provides information about each discrete symbol's start time and end time. In traditional demodulation methods, the speed and accuracy of symbol synchronization significantly impact the reception response speed and BER of digital wireless communication systems.

To analyze how symbol synchronization affects demodulation performance, we compare the BER performance between the proposed algorithm and the conventional methods at different symbol starting points, as shown in Fig.14. P=1 indicates that the starting point of the input data is the first bit of the signal (i.e., symbol synchronization). P=2 means that the demodulation starts from the second bit of the input

data (i.e., symbol-unsynchronized), P=Random (Because the number of sample points used in the simulation experiment is 4, so P = 1,2,3,4) means that the symbol starting position of the input data is randomly selected. We can see that the symbol-unsynchronized input data affects two demodulation algorithms' BER performance. Nevertheless, it has a more negligible impact on the R-FCN demodulator. Moreover, when the SNR is greater than or equal to 2 dB, the BER performance of the R-FCN demodulator for symbol-unsynchronized data is close to the traditional algorithm for symbol-synchronized signals. However, when the SNR is less than 0 dB, the CNN demodulator's BER performance (for symbol-unsynchronized signals) is worse than the conventional algorithm for all three modulation schemes. Besides, we see that from the two curves of P=2 and P=Random, the BER performance of the traditional demodulator is affected by the bit starting point. Nevertheless, the R-FCN demodulator is insensitive to the bit starting point. Specifically, a CNN-based R-FCN demodulator will obtain better robustness than the traditional demodulator.

V. CONCLUSION

In this paper, we have proposed a CNN-based architecture for demodulating the modulated signals by integrating CNN into the communication system. The proposed end-to-end R-FCN demodulator takes advantage of CNNs are superior in extracting high-level features, and ResNets address the problem of gradients vanishing. They are being used to improve the performance of the demodulator. Experiments show that the proposed R-FCN demodulator has better BER performance than conventional demodulators. In addition, we further investigate how symbol-unsynchronized data affect the demodulation performance for QPSK signals. Results show that the proposed demodulator is relatively insensitive to symbol-unsynchronized data compared to traditional methods.

REFERENCES

[1] S. Tsukamoto, K. Katoh, and K. Kikuchi, "Coherent demodulation of optical multilevel phase-shift-keying signals using homodyne detection and digital signal processing," *IEEE Photon. Technol. Lett.*, vol. 18, no. 10, pp. 1131–1133, May 26, 2006.

[2] R.-R. Chen, R. Koetter, U. Madhow, and D. Agrawal, "Joint noncoherent demodulation and decoding for the block fading channel: A practical framework for approaching Shannon capacity," *IEEE Trans. Commun.*, vol. 51, no. 10, pp. 1676–1689, Oct. 2003.

[3] Y. LeCun, Y. Bengio, and G. E. Hinton, "Deep learning," *Nature*, vol. 521, no. 7553, pp. 436–444, Dec. 2015.

[4] A. Patnaik, D. E. Anagnostou, R. K. Mishra, G. Christodoulou, and J. C. Lyke, "Applications of neural networks in wireless communications," *IEEE Antennas Propag. Mag.*, vol. 46, no. 3, pp. 130–137, Jun. 2004.

[5] M. Soltani, V. Pourahmadi, A. Mirzaei, and H. Sheikhzadeh, "Deep learning-based channel estimation," *IEEE Commun. Lett.*, vol. 23, no. 4, pp. 652–655, Apr. 2019.

[6] H. Ye, G. Y. Li, and B.-H. Juang, "Power of deep learning for channel estimation and signal detection in OFDM systems," *IEEE Wireless Commun. Lett.*, vol. 7, no. 1, pp. 114–117, Feb. 2018.

[7] T. J. O'Shea, T. Roy, and T. C. Clancy, "Over-the-air deep learning based radio signal classification," *IEEE J. Sel. Topics Signal Process.*, vol. 12, no. 1, pp. 168–179, Feb. 2018.

[8] S. Rajendran, W. Meert, D. Giustiniano, V. Lenders, and S. Pollin, "Deep learning models for wireless signal classification with distributed low-cost spectrum sensors," *IEEE Trans. Cogn. Commun. Netw.*, vol. 4, no. 3, pp. 433–445, Sep. 2018.

[9] Z. Zhang, C. Wang, C. Gan, S. Sun, and M. Wang, "Automatic modulation classification using convolutional neural network with features fusion of SPWVD and BJD," *IEEE Trans. Signal Inf. Process. Netw.*, vol. 5, no. 3, pp. 469–478, Sep. 2019.

[10] J. Wang, J. Li, H. Huang, and H. Wang, "Fine-grained recognition of error correcting codes based on 1-D convolutional neural network," *Digit. Signal Process.*, vol. 99, Apr. 2020, Art. no. 102668.

[11] B. Shen, H. Wu, and C. Huang, "Blind recognition of channel codes via deep learning," in *Proc. IEEE Global Conf. Signal Inf. Process. (GlobalSIP)*, Nov. 2019, pp. 1–5.

[12] E. Bourtsoulatze, D. B. Kurka, and D. Gunduz, "Deep joint source-channel coding for wireless image transmission," *IEEE Trans. Cognit. Commun. Netw.*, vol. 5, no. 3, pp. 567–579, Sep. 2019.

[13] S. Zheng, S. Chen, and X. Yang, "DeepReceiver: A deep learning-based intelligent receiver for wireless communications in the physical layer," *IEEE Trans. Cognit. Commun. Netw.*, vol. 7, no. 1, pp. 5–20, Mar. 2021.

[14] E. Nachmani, E. Marciano, L. Lugosch, W. J. Gross, D. Burshtein, and Y. Be'ery, "Deep learning methods for improved decoding of linear codes," *IEEE J. Sel. Topics Signal Process.*, vol. 12, no. 1, pp. 119–131, Feb. 2018.

[15] W. Xu, X. Tan, Y. Be'ery, Y.-L. Ueng, Y. Huang, X. You, and C. Zhang, "Deep learning-aided belief propagation decoder for polar codes," *IEEE J. Emerg. Sel. Topics Circuits Syst.*, vol. 10, no. 2, pp. 189–203, Jun. 2020.

[16] C. Cao, D. Li, and I. Fair, "Deep learning-based decoding of constrained sequence codes," *IEEE J. Sel. Areas Commun.*, vol. 37, no. 11, pp. 2532–2543, Nov. 2019.

[17] M. Li, H. Zhong, and M. Li, "Neural network demodulator for frequency shift keying," in *Proc. Int. Conf. Comput. Sci. Softw. Eng.*, 2008, pp. 843–846.

[18] X. Li, C. Zhao, and M. Jiang, "Neural network for demodulating the output signals of nonlinear systems with memory," in *Proc. 9th Int. Conf. Wireless Commun. Signal Process. (WCSP)*, 2017, pp. 1–5.

[19] Q. Wang, R. Liu, W. Wang, and G. Xie, "An electrocommunication system using FSK modulation and deep learning based demodulation for underwater robots," in *Proc. IEEE/RSJ Int. Conf. Intell. Robots Syst. (IROS)*, Oct. 2020, pp. 1699–1704.

[20] M. Önder, A. Akan, and H. Doğan, "Advanced neural network receiver design to combat multiple channel impairments," *TURKISH J. Electr. Eng. Comput. Sci.*, vol. 24, pp. 3066–3077, Apr. 2016.

[21] H. Wang, Z. Wu, S. Ma, S. Lu, H. Zhang, G. Ding, and S. Li, "Deep learning for signal demodulation in physical layer wireless communications: Prototype platform, open dataset, and analytics," *IEEE Access*, vol. 7, pp. 30792–30801, 2019.

[22] L. Zhang, H. Zhang, Y. Jiang, and Z. Wu, "Intelligent and reliable deep learning LSTM neural networks-based OFDM-DCSK demodulation design," *IEEE Trans. Veh. Technol.*, vol. 69, no. 12, pp. 16163–16167, Dec. 2020.

[23] K.-Z. Chen and A.-Q. Hu, "MPSK demodulation algorithm based on pattern recognition," in *Proc. Int. Conf. Neural Netw. Signal Process.*, Jun. 2008, pp. 182–186.

[24] D. Elbaz and M. Zibulevsky, "End to end deep neural network frequency demodulation of speech signals," 2017, *arXiv:1704.02046*.

[25] S. Ma, J. Dai, S. Lu, H. Li, H. Zhang, C. Du, and S. Li, "Signal demodulation with machine learning methods for physical layer visible light communications: Prototype platform, open dataset, and algorithms," *IEEE Access*, vol. 7, pp. 30588–30598, 2019.

[26] M. Zhang, Z. Liu, L. Li, and H. Wang, "Enhanced efficiency BPSK demodulator based on one-dimensional convolutional neural network," *IEEE Access*, vol. 6, pp. 26939–26948, 2018.

[27] X. Lin, R. Liu, W. Hu, Y. Li, X. Zhou, and X. He, "A deep convolutional network demodulator for mixed signals with different modulation types," in *Proc. IEEE 15th Int. Conf Dependable, Autonomic Secure Comput., 15th Int. Conf Pervasive Intell. Comput., 3rd Int. Conf Big Data Intell. Comput. Cyber Sci. Technol. Congress(DASC/PiCom/DataCom/CyberSciTech)*, Nov. 2017, pp. 893–896.

[28] M. Kozlenko, I. Lazarovych, V. Tkachuk, and V. Vialkova, "Software demodulation of weak radio signals using convolutional neural network," in *Proc. IEEE 7th Int. Conf. Energy Smart Syst. (ESS)*, May 2020, pp. 339–342.

[29] S. Dehdashtian, M. Hashemi, and S. Salehkaleybar, "Deep-learning-based blind recognition of channel code parameters over candidate sets under AWGN and multi-path fading conditions," *IEEE Wireless Commun. Lett.*, vol. 10, no. 5, pp. 1041–1045, May 2021.
[30] M. A. Hossain and M. S. A. Sajib, "Classification of image using convolutional neural network (CNN)," *Global J. Comput. Sci. Tech.*, vol. 19, no. 2, pp. 12–18, 2019.
[31] K. He, X. Zhang, S. Ren, and J. Sun, "Deep residual learning for image recognition," in *Proc. IEEE Conf. Comput. Vis. Pattern Recognit. (CVPR)*, Jun. 2016, pp. 770–778.
[32] A. L. Maas, A. Y. Hannun, and A. Y. Ng, "Rectifier nonlinearities improve neural network acoustic models," in *Proc. 30th Int. Conf. Mach. Learn. (ICML)*, 2013, pp. 1–6.
[33] X. Glorot and Y. Bengio, "Understanding the difficulty of training deep feedforward neural networks," *J. Mach. Learn. Res.*, vol. 9, pp. 249–256, May 2010.
[34] D. Kingma and J. Ba, "Adam: A method for stochastic optimization," in *Proc. Int. Conf. Learn. Represent. (ICLR)*, 2015, pp. 1–15.
[35] S. Ioffe and C. Szegedy, "Batch normalization: Accelerating deep network training by reducing internal covariate shift," 2015, *arXiv:1502.03167*.

WEN-JIE CHEN was born in 1989. She received the M.E. degree, in 2014. She is currently a Senior Engineer. Her research interest includes communication signal processing and analysis.

JIAO WANG received the B.S. degree in electronic information science and technology from China West Normal University, Nanchong, Sichuan, China, in 2016. She is currently pursuing the Ph.D. degree with the College of Electronic Science and Technology, University of Electronic Science and Technology of China (UESTC). Her research interests include wireless communications, signal processing, deep learning, and channel codes.

JIAN-QING LI (Member, IEEE) received the B.S. degree in electronics and information systems from Northeast Normal University, Changchun, Jilin, China, in 1998, and the Ph.D. degree in physical electronics from the University of Electronic Science and Technology of China (UESTC), Chengdu, Sichuan, China, in 2003. He is currently a Professor with UESTC. His research interests include deep learning, computer vision, and signal processing.